ISSCR

Adult Neural Progenitor Cells Transplanted into Spinal Cord Injury Differentiate into Oligodendrocytes, Enhance Myelination, and Contribute to Recovery

Sreenivasa Raghavan Sankavaram,[1,2,3] Ramil Hakim,[1,2] Ruxandra Covacu,[1,2,3] Arvid Frostell,[1] Susanne Neumann,[1,2] Mikael Svensson,[1,3] and Lou Brundin[1,2,3,*]

[1]Department of Clinical Neuroscience, Karolinska Institutet, 17177 Stockholm, Sweden
[2]Center of Molecular Medicine, Karolinska Institutet, 17177 Stockholm, Sweden
[3]Departments of Neurology and Neurosurgery, Karolinska University Hospital, 17176 Stockholm, Sweden
*Correspondence: lou.brundin@ki.se
 https://doi.org/10.1016/j.stemcr.2019.03.013

SUMMARY

Long-term survival and integration of neural progenitor cells (NPCs) transplanted following spinal cord injury (SCI) have been observed. However, questions concerning the differentiation choice, the mechanism of action, and the contribution of NPCs to functional recovery remains unanswered. Therefore, we investigated the differentiation of NPCs, global transcriptomal changes in transplanted NPCs, the effect of NPCs on neuroinflammation, and the causality between NPC transplantation and functional recovery. We found that NPCs transplanted following SCI differentiate mainly into oligodendrocytes and enhance myelination, upregulate genes related to synaptic signaling and mitochondrial activity, and downregulate genes related to cytokine production and immune system response. NPCs suppress the expression of pro-inflammatory cytokines/chemokines; moreover, NPC ablation confirm that NPCs were responsible for enhanced recovery in hindlimb locomotor function. Understanding the reaction of transplanted NPCs is important for exploiting their full potential. Existence of causality implies that NPCs are useful in the treatment of SCI.

INTRODUCTION

Traumatic spinal cord injury (SCI) is a devastating condition that often results in permanent and detrimental neurological deficits and reduced quality of life. Transplantation of stem cells have proven therapeutic potential in experimental studies (Ahuja et al., 2017; Curtis et al., 2018). Neural progenitor cells (NPCs) can be harvested from the subventricular zone (SVZ) in the mammalian brain (Doetsch et al., 1999). NPCs can self-renew and differentiate into neurons and glial cells (Morshead et al., 1994) as well as form neurospheres in the presence of epidermal growth factor (EGF) and basic fibroblast growth factor (bFGF) (Morshead et al., 1994; Reynolds and Weiss, 1992). NPCs transplanted into SCI survive (Akesson et al., 2007; Boido et al., 2011; Cummings et al., 2006; Jin et al., 2016; Karimi-Abdolrezaee et al., 2006; Macias et al., 2006; Nishimura et al., 2013; Okada et al., 2005; Pallini et al., 2005; Parr et al., 2007; Pfeifer et al., 2004, 2006; Piltti et al., 2013; Salazar et al., 2010; Sandhu et al., 2017; Vroemen et al., 2003), migrate (Karimi-Abdolrezaee et al., 2006; Mligiliche et al., 2005; Nishimura et al., 2013; Pallini et al., 2005; Salazar et al., 2010), integrate (Boido et al., 2011; Salazar et al., 2010; Vroemen et al., 2003), and form functional synapses with neurons and act as neuronal relays (Ben-Hur, 2010; Bonner et al., 2011; Cummings et al., 2005; Hong et al., 2014; Karimi-Abdolrezaee et al., 2006; Lu et al., 2012).

Conflicting results concerning the differentiation potential of transplanted NPCs have been reported. While differentiation into all neural lineages has been observed (Boido et al., 2011; Brock et al., 2017; Hong et al., 2014), some authors could only detect differentiation into astrocytes (Macias et al., 2006; Mligiliche et al., 2005; Pallini et al., 2005; Ricci-Vitiani et al., 2006; Sandhu et al., 2017). Specific differentiation into glia but not neurons has also been described (Karimi-Abdolrezaee et al., 2006; Parr et al., 2007; Pfeifer et al., 2004, 2006; Piltti et al., 2013; Salewski et al., 2015; Vroemen et al., 2003). Others have reported that transplanted NPCs differentiate into neurons and oligodendrocytes but not astrocytes (Cummings et al., 2006; Kumamaru et al., 2013; Salazar et al., 2010). A correlation between NPC transplantation and enhanced recovery of hindlimb locomotor function has been reported (Amemori et al., 2013; Ben-Hur, 2010; Cheng et al., 2016; Cummings et al., 2006; Hong et al., 2014; Karimi-Abdolrezaee et al., 2006; Li et al., 2014; Lu et al., 2012; Salazar et al., 2010; Salewski et al., 2015) (Boido et al., 2011; Cummings et al., 2006; Cusimano et al., 2012; Gu et al., 2012; Hofstetter et al., 2005; Kumamaru et al., 2013; Nishimura et al., 2013; Pallini et al., 2005). Enhanced angiogenesis through secretion of vascular endothelial growth factor (Li et al., 2014) and neurotrophic support have been proposed as explanatory models for the enhancement in recovery of hindlimb function (Amemori et al., 2013; Gu et al., 2012). Interactive synaptic reorganization between NPC-derived neurons in the recipient has also been proposed as a mechanism by which the NPCs enhance recovery of hindlimb locomotor function (Yokota et al., 2015).
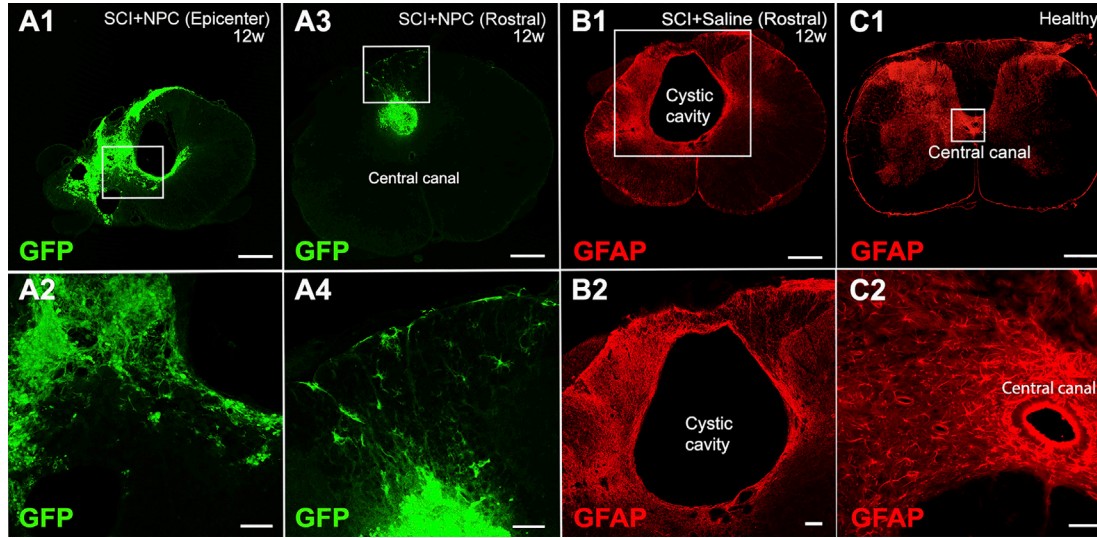
Figure 1. Engraftment of Transplanted NPCs

(A1–A4) (A1) Transversal section of an SCI epicenter containing transplanted GFP⁺ NPCs evaluated 12 weeks (w) following SCI. (A2) Enlargement of the delimitation in (A1). (A3) is comparable with (A1) but is taken rostral to the SCI epicenter. (A4) Enlargement of the delimitation indicated in (A3).

(B1 and B2) (B1) Transversal section rostral to the epicenter of an SCI subjected to saline injection, evaluated 12 weeks following SCI. (B2) Enlargement of the delimitation indicated in (B1).

(C1 and C2) (C1) Section of healthy spinal cord. (C2) Enlargement of the delimitation indicated in (C1).

Scale bars, 500 μm (A1, A3, B1, and C1), 100 μm (A2, A4, and B2), and 50 μm (C2). See also Figure S5.

Hence, the differentiation choice of NPCs following transplantation remains unclear. Moreover, an unbiased analysis of the transcriptome of transplanted NPCs has, to our knowledge, never been conducted. Although an indication of correlation between transplantation of NPCs and recovery in hindlimb locomotor function exists, neither the causality nor the mechanism of action has been investigated, proved, or reported on.

In this study, we investigated global transcriptomal changes in transplanted NPCs, the presence of a causal relationship between NPC transplantation and recovery in hindlimb locomotor function, NPC differentiation, and NPC effects on neuroinflammation.

RESULTS

Transplanted NPCs Differentiate into Oligodendrocytes and Enhance Myelination

Eighty-three percent (confidence interval [CI] 75%–91%) of undifferentiated NPCs expressed SOX2 transcription factor *in vitro* (Figures S1A1–SA3 and S1E). NPCs differentiated *in vitro* expressed TuJ1 (neuron-specific class III β-tubulin) and glial fibrillary acidic protein (GFAP) (Figures S1B1–S1E). The fate of transplanted NPCs/neurospheres was investigated in terms of survival, integration, migration,

and differentiation. Survival rate of transplanted NPCs was estimated to be ~25%. GFP⁺ NPCs were detected rostral to and in the epicenter of the SCI at 12 weeks following transplantation (Figures 1A1–1A4). The NPCs filled the cystic cavity (Figures 1A3 and 1A4). A cystic cavity was formed and prevailed in animals that received saline injection (Figures 1B1 and 1B2). At 12 weeks following transplantation into SCI, 6% (CI 4%–9%) of the NPCs engrafted in the epicenter expressed SOX2 (Figures S2A1–S2A4 and 2E) and hardly any transplanted NPCs expressed Nestin (Figures S2B1–S2B4), suggesting that the majority of NPCs lost their stem cell characteristics. Transplanted NPCs expressed GFAP (25%; 95% CI 22%–30%) rostral to (Figures 2A1–2B4 and 2E) and in the injury epicenter (Figures S2C1–S2C9) at 12 weeks post SCI, suggesting astrocytic differentiation. Engrafted NPCs expressed TuJ1 to a low extent (2%; 95% CI 0%–4%) (Figures 2C1–2D4 and 2E) at 12 weeks post SCI. Fifty-two percent (95% CI 46%–59%) of the transplanted NPCs expressed CC1, suggesting oligodendrocyte differentiation (Figures 3A1–3A4 and S3A1–S3A3). Transplanted NPCs also expressed OLIG2 (Figures 3B3–3B5 and S3B1–S3B4) and 2′,3′-cyclic nucleotide 3′-phosphodiesterase (CNPase) (Figures 3C1–3C5 and S4A1–S4A4), and a high density of myelin basic protein (MBP) was detected in the area where engrafted NPCs were detected (Figures 3D1–3D6, 3E1–3E4, and
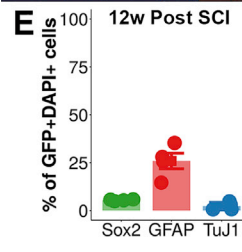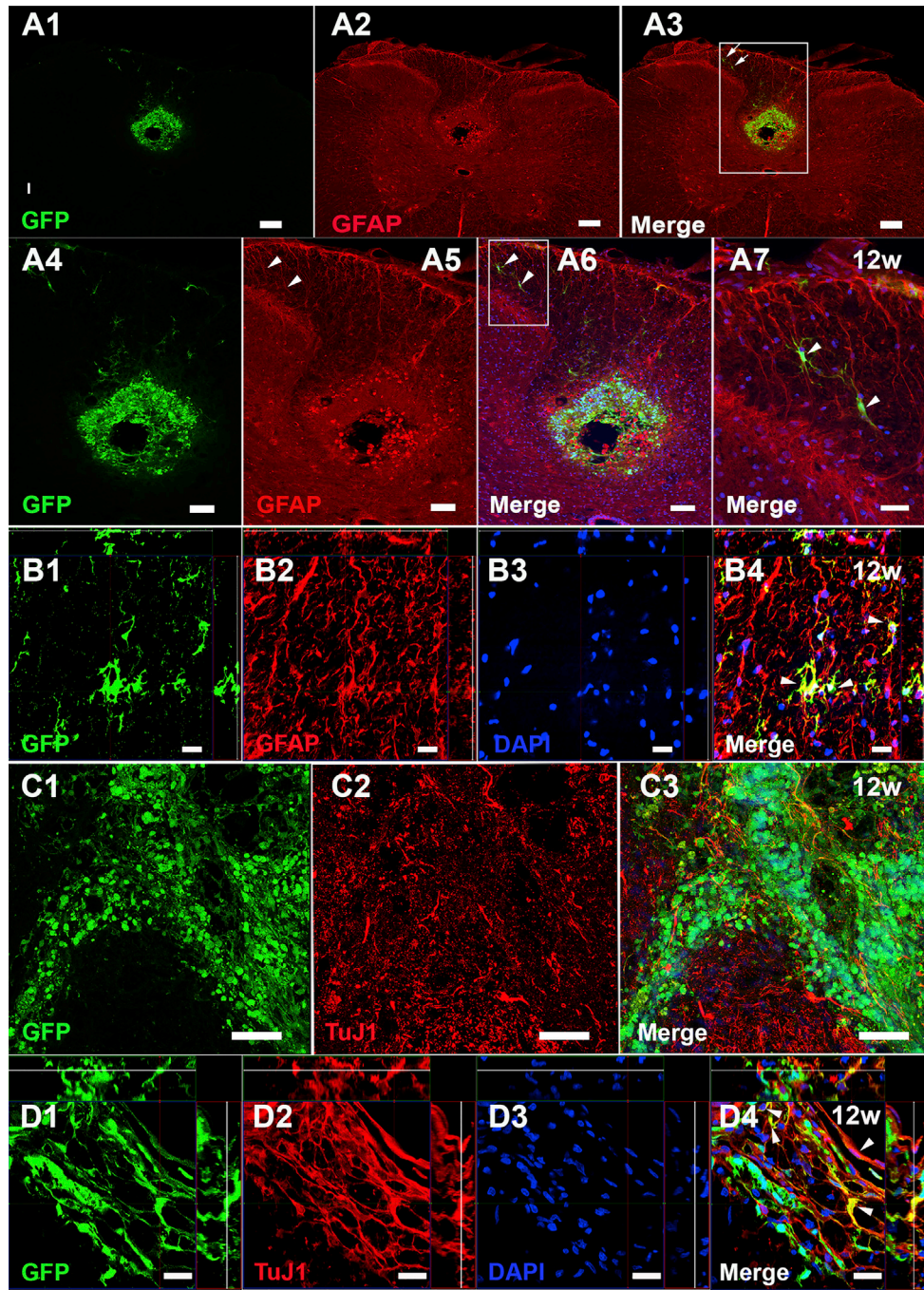
(legend on next page)

S4B1–S4B5). No difference in differentiation profile of transplanted NPCs could be detected along the rostral/caudal axis or the dorsal/ventral axis. RNA sequencing (Figure 3F) and Luxol fast blue staining (Figure 3G) confirmed the oligodendrocyte differentiation and enhanced myelination. Transplanted NPCs were detected predominantly in the white matter (Figures S5A1–S5B3), but occasional homogeneous spreading in both gray and white matter was also detected (Figures S5C and S5D). The transplanted NPCs showed a tendency to migrate along the caudal/cranial axis (~2 mm/week) (Figures S5E1–S5E3). Transplanted NPCs did not express activated form of caspase-3, suggesting that NPCs do not undergo apoptosis in the recipient (Figures S6A1–S6B4). Taken together, transplanted NPCs survived, integrated, migrated, filled the cystic cavity, and differentiated mainly into oligodendrocytes and enhanced myelination within the recipient spinal cord.

Transplanted NPCs Upregulate Genes Related to Synaptic Signaling and Mitochondrial Activity, and Downregulate Genes Related to Cytokine Production and Immune System Response

Global transcriptomal changes in NPCs/neurospheres sorted 3 and 4 weeks following transplantation were investigated (Figures S7A–S7D). The time points were chosen to characterize the transcriptional changes in NPCs induced by the acute and subacute injury environment (Figure 4A). We found a substantial separation between NPCs transplanted into injured spinal cord (SCI+NPCs), NPCs transplanted into uninjured spinal cord (naive+NPCs), and non-transplanted NPCs (in vitro+NPCs) (Figures 4B–4F). At 3 weeks post SCI, SCI+NPCs as compared with naive+NPCs upregulated genes related to synaptic signaling, mitochondrial activity, and cell-cycle progression while they downregulated genes related to cytokine production, immune system response, and cell migration (Figure 4G; Tables S1 and S2). At 4 weeks post SCI, SCI+NPCs as compared with naive+NPCs also upregulated genes related to synaptic signaling and downregulated genes related to cell adhesion, cellular response to stimuli, and microtubule/cytoskeleton (Figure 4G; Tables S1 and S2). At both time points the synaptic signaling was defined by gene ontology (GO) terms such as *Signal release from synapse (GO:0099643)* and *Synap-*

tic transmission, GABAergic (GO:0051932), indicating an upregulation of inhibitory synaptic signaling in the NPCs, induced by the injury environment. The cytokine production was defined by GO terms such as *Interleukin-6 production (GO:0032635)* and *Interleukin-1 beta production (GO:0032611)*, indicating suppression of production of pro-inflammatory cytokines by NPCs. SCI+NPCs as compared with naive+NPCs upregulated GO terms related to myelination and oligodendrocytes at both 3 and 4 weeks post SCI: *Myelin sheath (GO:0043209)* and *Oligodendrocyte development (GO:0014003)* (Figure 3F and Table S3). Highly differentially expressed genes from these GO terms related to myelination were *Atp1a3*, *Cntn1*, *Dnm1*, *Erbb2*, *Ina*, and *Uchl1* (Figures S7E and S7G), and from GO terms related to oligodendrocyte development were *Ascl1*, *Nkx2-2*, *Hes5*, and *Tcf7l2* (Figures S7 F and S7H). Taken together, SCI+NPCs upregulate genes related to synaptic signaling and mitochondrial activity in general and specifically genes related to myelination and oligodendrocytes, while they downregulate genes related to cytokine production and immune system response.

Transplanted NPCs Suppress Expression of Pro-inflammatory Cytokines/Chemokines

The inflammatory response following SCI was investigated by analyzing the expression of pro-inflammatory cytokines/chemokines in cerebrospinal fluid (CSF) (Figure 5A). At 3 weeks post SCI, the animals that received NPCs/neurospheres (SCI+NPC) had a lower expression of pro-inflammatory cytokines/chemokines in comparison with SCI+saline animals ($p < 0.05$) (Figure 5B). This result was robust in bootstrap sensitivity analysis (Figure 5C). The difference at 3 weeks was explained by significant differences in interleukin-1a (IL-1a), IL-1b, IL-2, tumor necrosis factor α, GRO/KC (growth-regulated oncogene/keratinocyte chemoattractant), monocyte chemotactic protein 1, and macrophage inflammatory protein 1a (Figures 5D and 5E). No difference in pro-inflammation could be detected between the treatments at 6 and 12 weeks post SCI (Figure 5E). Gene expression of cytokine/chemokines is presented in Figures S6D1–S6D3. Taken together, NPCs transplanted into SCI suppress the pro-inflammatory response at 3 weeks post SCI.

Figure 2. Expression of GFAP and TuJ1 in Transplanted NPCs
(A) (A1–A3) Transversal section rostral to an SCI epicenter containing transplanted GFP+ NPCs, evaluated 12 weeks (w) following injury. (A4–A6) Reports and enlargement of the delimitation indicated in (A3). (A7) Enlargement of the delimitation indicated in (A6). Arrows mark GFP+GFAP+NPCs.
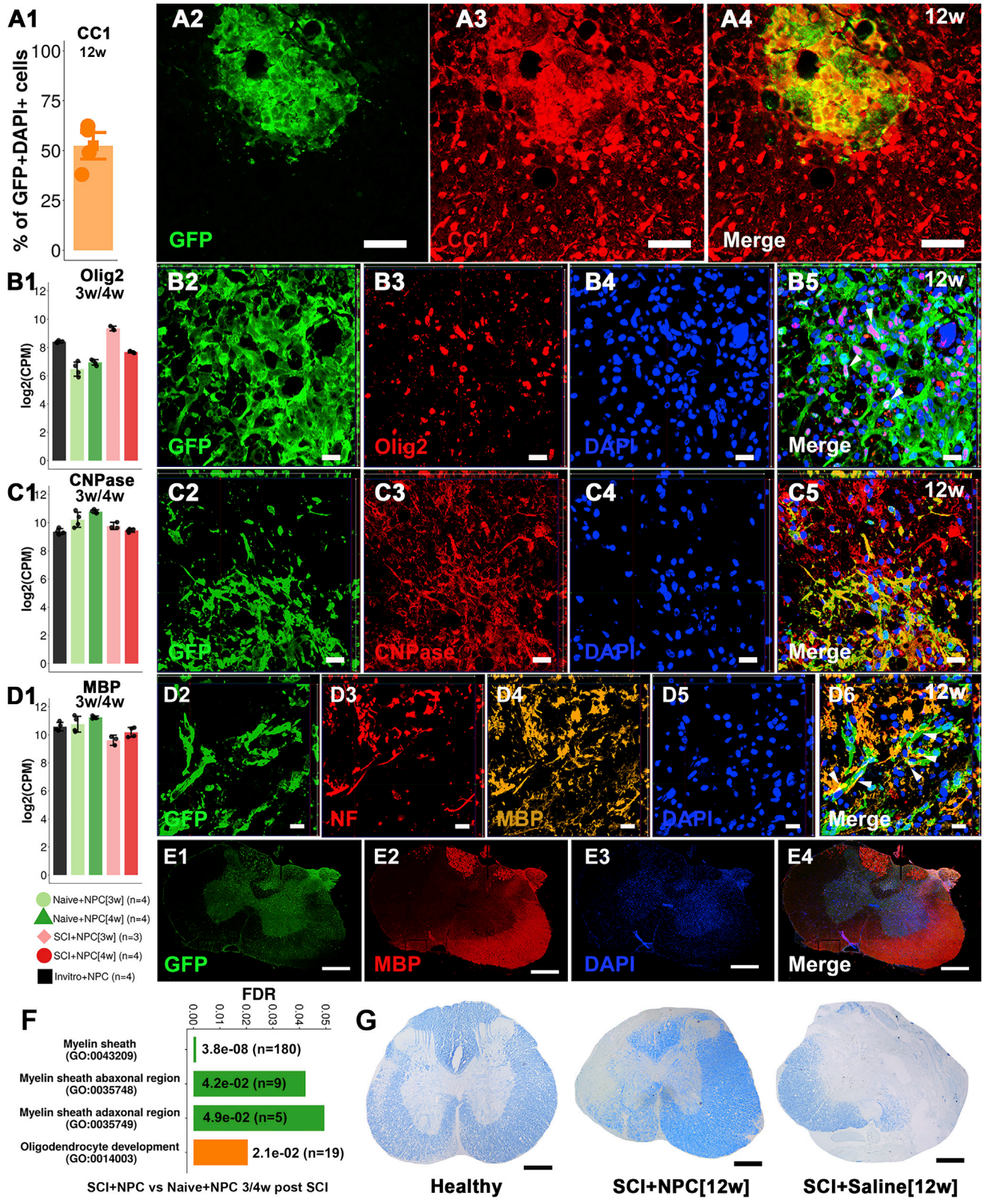(B) Orthogonal projections (B1–B4).
(C) Transversal section of a spinal cord dorsal horn rostral to an SCI epicenter evaluated 12 weeks post SCI (C1–C3).
(D) Orthogonal projections (D1–D4).
(E) Mean percentage of co-localization. Mean is surrounded a by 95% CI. Each dot represents one animal.
Scale bars, 200 μm (A1–A3), 100 μm (A4–A6 and C1–C3), 50 μm (A7), and 20 μm (B1–B4 and D1–D4). See also Figures S1, S2, and S5.

A1 CC1 12w
% of GFP+DAPI+ cells

A2 GFP
A3 CC1
A4 Merge 12w

B1 Olig2 3w/4w
log2(CPM)

B2 GFP
B3 Olig2
B4 DAPI
B5 Merge 12w

C1 CNPase 3w/4w
log2(CPM)

C2 GFP
C3 CNPase
C4 DAPI
C5 Merge 12w

D1 MBP 3w/4w
log2(CPM)

D2 GFP
D3 NF
D4 MBP
D5 DAPI
D6 Merge 12w

Naive+NPC[3w] (n=4)
Naive+NPC[4w] (n=4)
SCI+NPC[3w] (n=3)
SCI+NPC[4w] (n=4)
Invitro+NPC (n=4)

E1 GFP
E2 MBP
E3 DAPI
E4 Merge

F FDR

Myelin sheath (GO:0043209) — 3.8e-08 (n=180)
Myelin sheath abaxonal region (GO:0035748) — 4.2e-02 (n=9)
Myelin sheath adaxonal region (GO:0035749) — 4.9e-02 (n=5)
Oligodendrocyte development (GO:0014003) — 2.1e-02 (n=19)

SCI+NPC vs Naive+NPC 3/4w post SCI

G Healthy   SCI+NPC[12w]   SCI+Saline[12w]

(legend on next page)

Transplanted NPCs Enhance Recovery of Hindlimb Locomotor Function

Recovery of hindlimb locomotor function following SCI was evaluated using the Basso, Beattie, and Bresnahan (BBB) locomotor rating scale and by kinematic analysis (Figure 6A). Animals that received NPCs/neurospheres (SCI+NPC) improved in BBB score over time (p < 0.001), while no statistically significant improvement in animals that received saline (SCI+saline) could be detected over time using repeated-measures analysis (p = 0.82) (Figure 6B). At 12 weeks post SCI, the SCI+NPC animals had an average BBB score of 15.0 (95% CI 13.4–16.6), while SCI+saline animals had a significantly lower average score of 8.5 (95% CI 3.4–13.6) (p < 0.05). At 12 weeks post SCI the SCI+NPC animals had an iliac crest height (ICH) similar to that of healthy animals, which was significantly higher than that of SCI+saline animals (p < 0.05) (Figure 6C). We detected that SCI+NPC animals took significantly fewer forelimb steps at 3, 6, and 12 weeks post SCI compared with SCI+saline animals (p < 0.05) (Figure 6D). At 12 weeks post SCI the SCI+NPC animals had on average a longer protraction distance compared with SCI+saline animals (p < 0.05) while the opposite was true for retraction (p < 0.05) (Figure 6E). SCI+NPC animals had a narrower stride width at 12 weeks post SCI compared with SCI+saline animals (p < 0.05) (Figure 6F). The stride length for the SCI+NPC animals was longer at 12 weeks post SCI compared with SCI+saline animals (p < 0.05) (Figure 6G). The coordination of paw placement of SCI+NPC animals normalized to the level of healthy controls at 12 weeks, which was not the case for SCI+saline animals (Figure 6H). Taken together, animals that received transplantation of NPCs following SCI had a superior recovery in hindlimb locomotor function in comparison with that of animals injected with saline.

A Causal Relationship Exists between NPC Transplantation and Enhanced Recovery in Hindlimb Locomotor Function

Existence of causality between transplantation of NPCs/neurospheres and enhanced recovery of hindlimb locomotor function was investigated by eliminating NPCs immediately following transplantation using diphtheria toxin (DT) (Figures 7A and 7B). Transfected GFP[+] NPCs expressed mCherry *in vitro* and in the recipient (Figures 7D1–7D4).

Following administration of DT the GFP[+] NPCs were ablated and were eventually engulfed by Iba1^{+} cells (Figures 7E1–7E4). SCI+NPC animals did not have a significantly lower level of pro-inflammation in comparison with SCI+NPC&DT (Figure 7F). At 6 weeks post SCI, the SCI+NPC animals had a BBB score that was significantly higher than that of SCI+NPC&DT animals (p < 0.05) (Figure 7G). At 6 weeks post SCI, the SCI+NPC animals had a significantly higher ICH in comparison with the SCI+NPC&DT animals (p < 0.05) (Figure 7H). Taken together, there is a causal relationship between transplantation of NPCs and enhanced recovery of hindlimb locomotor function following SCI.

DISCUSSION

In this study we found that NPCs transplanted into SCI differentiate into oligodendrocytes and enhance myelination, upregulate genes related to synaptic signaling and mitochondrial activity, and downregulate genes related to cytokine production and immune system response. Furthermore, NPCs suppress pro-inflammation and are responsible for enhanced recovery in hindlimb locomotor function.

The enhanced recovery in locomotor function following NPC transplantation has been reported repeatedly previously (Amemori et al., 2013; Ben-Hur, 2010; Cheng et al., 2016; Cummings et al., 2006; Hong et al., 2014; Karimi-Abdolrezaee et al., 2006; Li et al., 2014; Lu et al., 2012; Salazar et al., 2010; Salewski et al., 2015) (Boido et al., 2011; Cummings et al., 2006; Cusimano et al., 2012; Gu et al., 2012; Hofstetter et al., 2005; Kumamaru et al., 2013; Nishimura et al., 2013; Pallini et al., 2005). In this study, in addition to enhanced locomotor function we also showed that the animals improved in terms of coordination, muscle regeneration, step cycle process, and stepping pattern, and had enhanced hindlimb support following SCI. Moreover, the immediate ablation of NPCs resulted in a BBB score and ICH similar to those of injury control and saline-injected animals, proving a causal relationship between transplantation of NPCs and enhanced recovery in hindlimb function. Although ablation of transplanted NPCs has been done previously (Cummings et al., 2005; Fujimoto et al., 2012), this was investigated in either human NPCs or

---

Figure 3. Expression of Oligodendrocyte and Myelin Markers in Transplanted NPCs

(A) (A1) Quantification of co-localization. (A2–A4) Transversal section of a dorsal horn rostral to an SCI epicenter containing NPCs.

(B–D) (B1, C1, D1) Gene expression reported using log$_2$(counts per million) in sorted GFP[+] NPCs. (B2–B5, C2–C5, D2–D6) Orthogonal projections of transversal sections rostral to SCI epicenter.

(E) Transversal section rostral to an SCI (E1–E4).

(F) Gene ontology terms reporting average (of two contrasts) false discovery rate (FDR) and number of genes (n) for each term.

(G) Luxol fast blue staining of spinal cord (epicenter) sections.

Scale bars, 500 μm (E1–E4 and G), 50 μm (A2–A4), and 20 μm (B2–D6). See also Figures S3–S5.
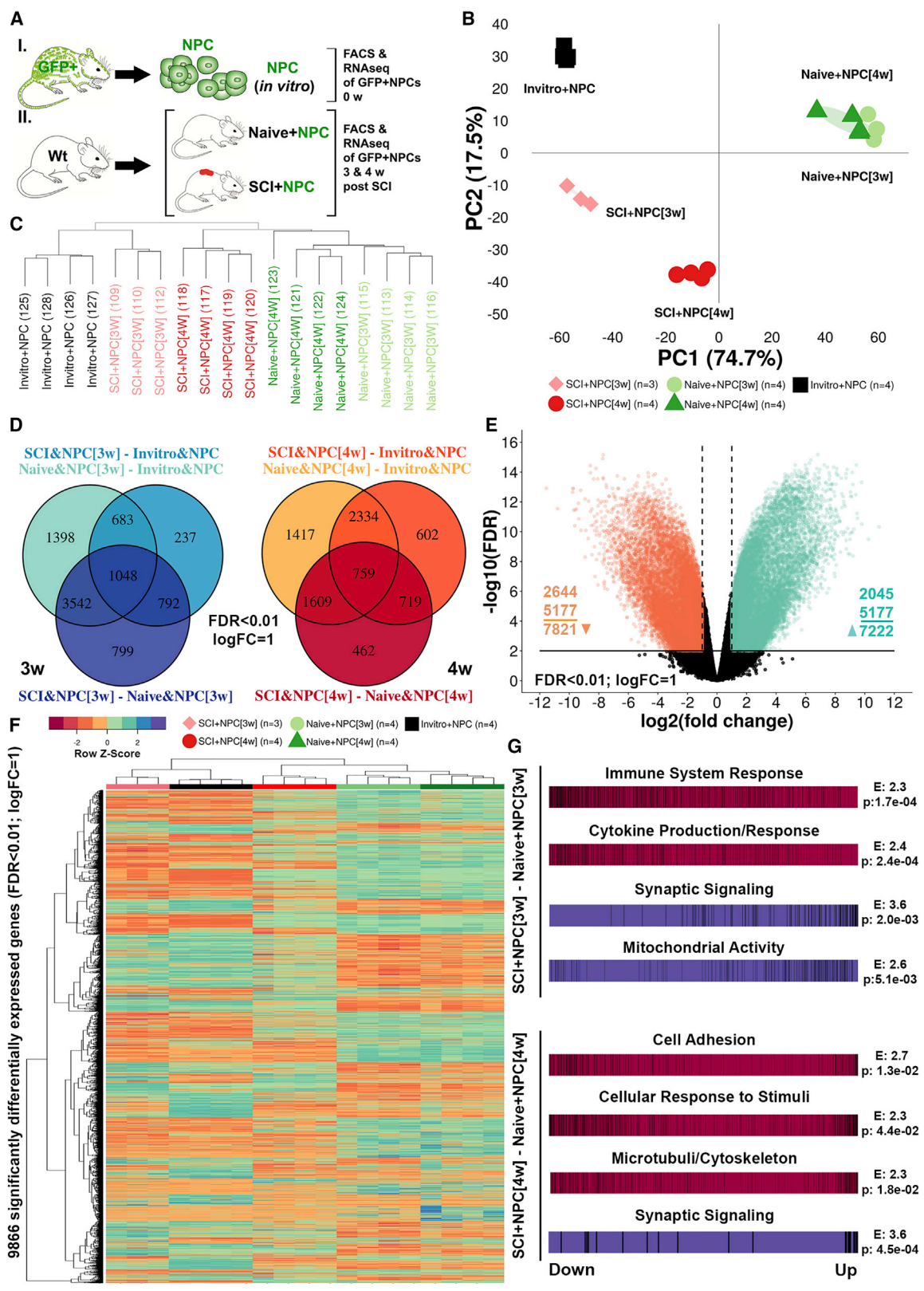
(legend on next page)

induced pluripotent stem cells, in moderate contusion SCI, and/or in the chronic phase of SCI, in contrast to our study, which investigated severe contusion SCI using adult NPCs from littermates in the acute/subacute phase of SCI. This study focused on hindlimb motor function, which is perhaps the most obvious deficit following SCI, but did not cover the sensory and/or autonomic functions, which are equally relevant deficits occurring following SCI. Thus, upcoming studies might be able to contribute by focusing more on the latter topics using an ablation approach. In conclusion, we found a causal relationship between transplantation of NPCs and enhanced recovery of hindlimb motor function.

We found that NPCs at 3 weeks following transplantation into SCI upregulated genes related to synaptic signaling and downregulated genes promoting cytokine production. The upregulation of synaptic signaling might support the theory proposed by Ben-Hur (2010), among others, that NPCs transplanted into SCI restore synaptic connectivity and reconstruct neural circuits (Ben-Hur, 2010; Bonner et al., 2011; Cummings et al., 2005; Hong et al., 2014; Karimi-Abdolrezaee et al., 2006; Lu et al., 2012). Downregulation of cytokine production was in line with the suppression of cytokines/chemokines detected in the CSF. Both the synaptic signaling and the lower levels of pro-inflammatory cytokines might have contributed to the enhanced functional recovery observed. Moreover, NPCs transplanted into SCI upregulated genes related to myelination and oligodendrocytes at 3 and 4 weeks post SCI. This was in line with the significant oligodendrocyte differentiation (CC1, OLIG2) and enhanced myelination (CNPase, MBP) of axons observed using histology at 12 weeks post SCI. The enhanced myelination mediated by the newly formed oligodendrocytes might at least partially, in combination with the fact that the NPCs filled the cystic cavity, explain the enhanced functional recovery. Genes related to apoptosis were downregulated, which was in line with the complete lack of caspase-3-positive NPCs and the extensive survival of NPCs observed at 12 weeks post SCI. The long-term survival confirms what Akesson et al. (2007) and Vroemen et al. (2003), among others, have already reported (Akesson et al., 2007; Boido et al., 2011; Cummings et al., 2006; Jin et al., 2016; Kar-

imi-Abdolrezaee et al., 2006; Macias et al., 2006; Nishimura et al., 2013; Okada et al., 2005; Pallini et al., 2005; Parr et al., 2007; Pfeifer et al., 2004, 2006; Piltti et al., 2013; Salazar et al., 2010; Sandhu et al., 2017; Vroemen et al., 2003). The littermate approach implemented might partially explain the long-term survival and high level of integration of NPCs. Previous studies investigating global transcriptional analysis following NPC transplantation has sequenced the entire spinal cord tissue (and not only the NPCs) (Nishimura et al., 2013) or the NPCs were sequenced but in the acute phase (7 days) of SCI following acute transplantation (Kumamaru et al., 2012), in contrast to this study, which sequenced only NPCs at 3 and 4 weeks post SCI following transplantation in the subacute phase. In conclusion, NPCs transplanted following SCI survive, differentiate into oligodendrocytes and enhance myelination, suppress neuroinflammation, and seem to upregulate synaptic signaling, which are all plausible explanations for the enhanced recovery of hindlimb motor function mediated by the NPCs.

Transplanted NPCs differentiated not only into oligodendrocytes but also into astrocytes. The obvious risk of astrocytic differentiation is a potential addition and contribution to the glial scar. The size of the glial scar, however, was not investigated in this study. Although the transplanted NPCs did enhance recovery in hindlimb locomotor function, a lower level of astrocytic differentiation could perhaps have resulted in a more significant recovery. Our findings, indicating that transplanted NPCs have the potential to differentiate into all major cell types in the CNS, reflects what Boido et al. (2011) and others also found to be true for transplanted NPCs (Boido et al., 2011; Brock et al., 2017; Hong et al., 2014). However, our data are more in line with reports indicating that glial cell differentiation is more prevalent than differentiation into neural cells (Karimi-Abdolrezaee et al., 2006; Macias et al., 2006; Mligiliche et al., 2005; Pallini et al., 2005; Parr et al., 2007; Pfeifer et al., 2004, 2006; Piltti et al., 2013; Ricci-Vitiani et al., 2006; Salewski et al., 2015; Sandhu et al., 2017; Vroemen et al., 2003). The difference in differentiation preference of NPCs taken from different CNS sites has been demonstrated by us (Covacu et al., 2014) and others (Kulbatski and Tator, 2009). In homeostatic condition, the spinal

Figure 4. Global Transcriptomal Changes in Transplanted NPCs
(A) Experimental design.
(B) Biological replicates following principal component analysis.
(C) Agglomerative hierarchical clustering of biological replicates.
(D) Venn diagrams reporting the number of significantly differentially expressed genes (FDR < 0.01, log_{FC} = 1) for relevant contrasts.
(E) Volcano plot of significantly differentially expressed genes (FDR < 0.01, log_{FC} = 1) for all contrasts in (D).
(F) Heatmap representation of significantly differentially expressed genes (FDR < 0.01, log_{FC} = 1).
(G) Barcode plots for top functional categories presented with enrichment score (E) and FDR (p) following competitive gene set testing.
See also Figure S7.
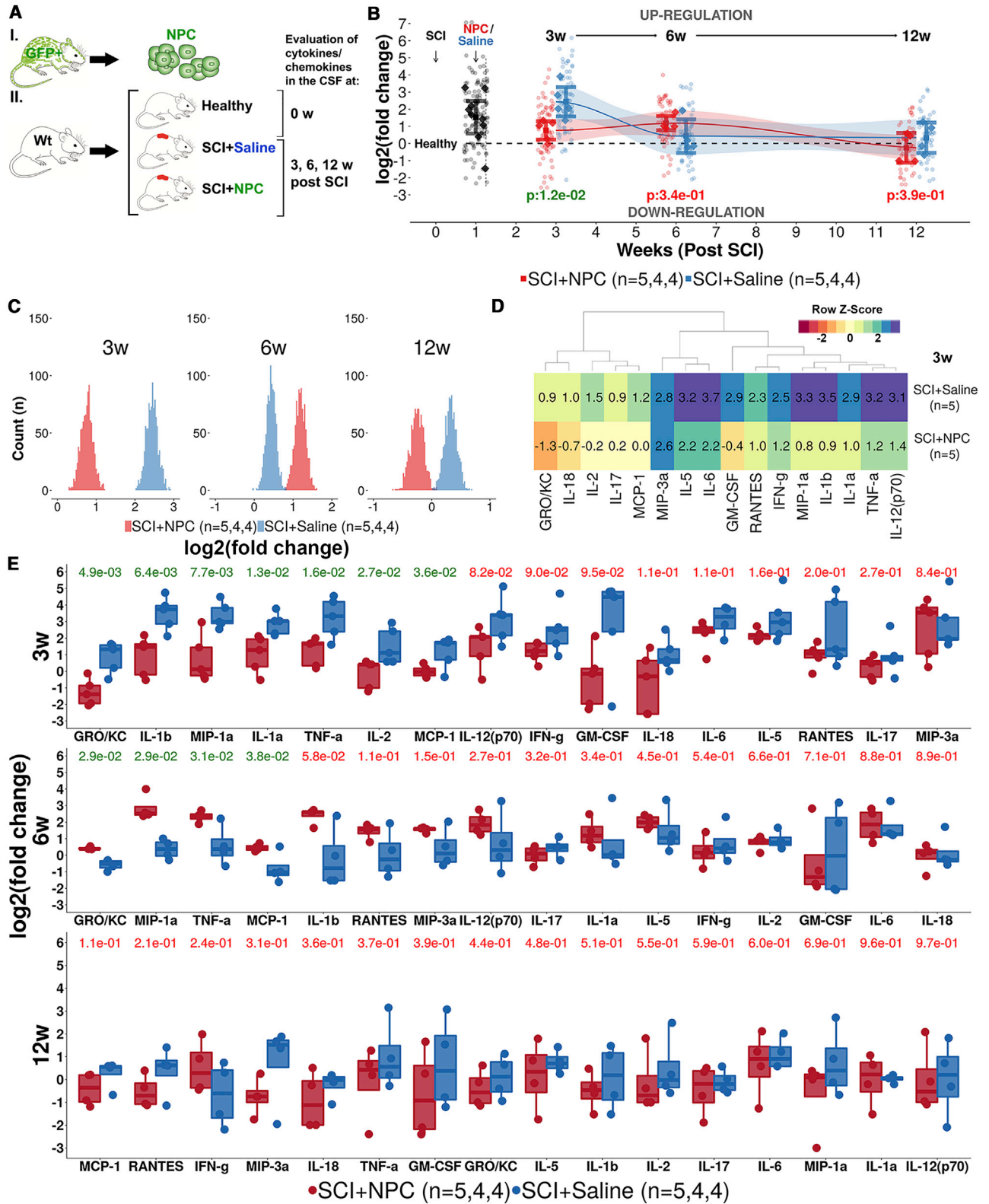
(legend on next page)

cord (SC)-derived NPCs are more gliogenic while the brain-derived NPCs are more neurogenic. However, when exposed to inflammation the differentiation outcome of the NPCs from different sites changes. Following exposure to inflammation, the SC-NPCs tend to increase their neurogenic differentiation (Covacu et al., 2014) while the differentiation in the SVZ is preferentially gliogenic (Tepavčević et al., 2011). Tepavčević et al. (2011) demonstrated that following experimental autoimmune encephalomyelitis the SVZ differentiation profile is skewed toward oligodendrogenesis, where the proliferation of pro-oligodendrogenic transit amplifying population expressing Olig2 and Dlx-2 is favored. In concordance with that study, we report that the SVZ-NPCs transplanted into inflamed spinal cord are preferentially differentiating into oligodendrocytes, although some differentiation into astrocytes was observed.

The suppression of neuroinflammation early on following SCI indicates that the NPCs can affect/modulate the macrophage response. This is in line with the findings in the global transcriptional analysis in which the NPCs 3 weeks post SCI managed to downregulate genes related to cytokine production but also to downregulate genes related to immune system response. This, however, was not true at 4 weeks post SCI, which is also in line with the protein expression of cytokines/chemokines in the CSF at 3–6 weeks post SCI. We do not know of any study reporting an extensive evaluation of the protein expression of cytokines/chemokines in the CSF and thus lack a proper benchmark for our data. Unfortunately, neither the gene expression nor the protein expression analysis allowed us to determine the mechanism of the suppressive effect on the inflammation mediated by the NPCs.

The results of this study are valid for severe contusion SCI in rodents using a littermate approach for NPC transplantation in the subacute phase of SCI. In terms of reproducibility, the accuracy of the transplantations is of great importance for proper placement of the NPCs in the spinal cord. In terms of clinical use, there are a few hurdles to overcome. First, this experimental setup requires NPCs to be harvested from the SVZ. In a clinical setting, tissue matching might reduce graft rejection but a sufficient number of

NPCs might be challenging to obtain. Second, in this study the NPCs were transplanted 8–10 days post SCI. However, NPCs require weeks of culturing following harvesting before they can be transplanted.

In summary, NPCs transplanted following SCI differentiate mainly into oligodendrocytes, upregulate genes related to synaptic signaling and mitochondrial activity, and downregulate genes related to cytokine production and immune system response. NPCs suppress the expression of pro-inflammatory cytokines/chemokines, and NPCs are responsible for enhanced recovery in hindlimb locomotor function.

EXPERIMENTAL PROCEDURES

Animals, Breeding, and Genotyping

Lewis rats heterozygous for enhanced green fluorescent protein (eGFP) under the ubiquitin C promoter on chromosome 5 (LEW-Tg(EGFP)455Rrrc) were bought through RRRC (Rat Research Resource Center, Columbia). A littermate approach was implemented in which NPCs were established from an eGFP carrier and transplanted to an eGFP non-carrier littermate. All animal experiments were approved by the local ethical committee (N38/16, N196/15, N12317/17).

Neural Progenitor Cells

Harvesting and Culturing

NPCs were isolated from the SVZ of adult eGFP carrier rats (Johansson et al., 1999). In brief, rats were euthanized and the SVZ was identified and removed. The SVZ was dissociated using papain (Worthington, LS003126). Following washing in Leibovitz's 15 medium (Life Technologies #31415086), the NPCs were cultured in growth medium (DMEM/F-12 medium [Gibco #31331093] supplemented with B27 [Gibco #17504044], 100 U/mL Pen-Strep [Sigma #15140122], 20 ng/mL EGF [Sigma E4127], and 10 ng/mL bFGF [R&D Systems #3339-FB]) and were passaged two times.

Experimental Spinal Cord Injury

Rats were anesthetized using 4% isoflurane (Baxter) with 30% O_2 in combination with the subcutaneous (s.c.) administration of 0.05 mg/kg buprenorfin (Temgesic; Indivior, 0.3 mg/mL) and 5 mg/kg karprofen s.c. (Rimadyl vet.; Orion Pharma Animal Health, 50 mg/mL). Animals were weighed, received 4 mL of

---

Figure 5. Expression of Pro-inflammatory Cytokines/Chemokines in the Cerebrospinal Fluid

(A) Experimental design.

(B) Level of pro-inflammation as $\log_2$(fold change) in relation to expression in healthy animals. Mean is surrounded by a 95% CI. Each diamond represents one animal. Each dot represents one cytokine/chemokine. p values for two-group comparison are presented at each time point.

(C) Histograms of bootstrapped replicates (1,000 runs) of the level of pro-inflammation per treatment group.

(D) Heatmap representation of the mean $\log_2$(fold change) in comparison with healthy control per treatment and cytokine 3 weeks (w) post SCI.

(E) Expression of cytokines/chemokines as $\log_2$(fold change) in relation to healthy control. Each dot represents one animal. p values for two-group comparison are presented for each time point and cytokine/chemokine.

See also Figure S6.
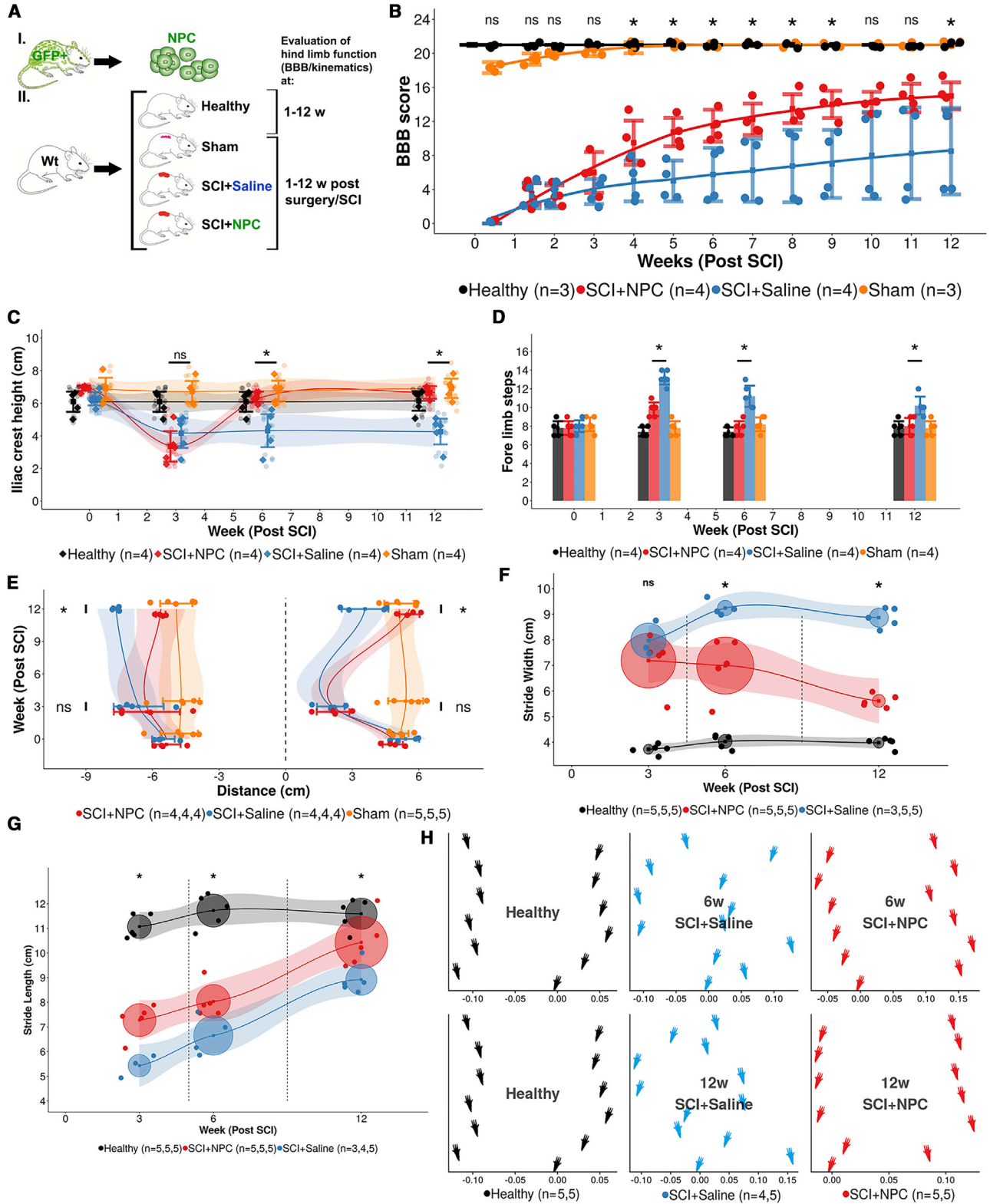
(legend on next page)

normal saline s.c., and their eyes were covered with ointment (Oculentum simplex; APL). A longitudinal skin incision was made above the thoracic spine on the dorsal side of the animal. The muscles were carefully separated, and the spinal column was stabilized using bilateral fixators in a stereotaxic frame (Kopf 900&900-C). Laminectomy was performed using a surgical drill (Anspach eMax 2) at Th11. The rat was placed under a spinal cord impactor (Infinite Horizon, IH-0400), and a 200-kdyn contusion SCI was delivered. The skin was sutured using 4.0 Vicryl (Ethicon). Buprenorfin was administrated twice daily and karprofen once daily during the 3 days following surgery using the same doses given at induction. Urine bladders were manually compressed until the rats recovered reflexive bladder emptying. Rats were weighed weekly, and a maximum weight loss of 25% was accepted.

Transplantation of Neural Progenitor Cells

NPCs were transplanted into the SCI epicenter at 8–10 days post SCI induction. During days 1–3 prior to transplantation, the animals were given 10 mg/kg cyclosporine (Sandimmun; Novartis) s.c. once daily. NPCs were collected from culture by centrifugation at $300 \times g$, placed in Eppendorf tubes with a small amount of PBS, and kept on ice. Routines for anesthesia, analgesics, and preoperative and intraoperative procedures used in SCI surgery were implemented. The spinal cord was re-exposed. The spinal column was stabilized in a stereotaxic frame. A glass capillary needle was attached to a Hamilton syringe (Hamilton 80330), which in turn was attached to a holder in the stereotaxic frame. The glass capillary was inserted 1.5 mm into the spinal cord and the cell suspension was injected slowly. A total of 500,000–600,000 NPCs, in 6 μL of PBS, were transplanted as single cells or neurospheres into the epicenter of the SCI. NPCs were transplanted into the injury epicenter with the intent to replace injured and/or lost cells at the location were the loss was the largest and modulate the inflammation response in the lesion site. Furthermore, transplantation into the injury epicenter allows for potential filling of the cystic cavity which, in combination with oligodendrocyte differentiation, could potentially enhance the myelination of outgrowing axons. The skin was sutured and postoperative procedures implemented.

Active Elimination of Engrafted Neural Progenitor Cells

NPCs were transfected with a non-integrating, self-replicating enhanced episome vector (EEV; System Biosciences #EEV600A-1) containing the cDNA sequence of the human heparin-binding EGF-like growth factor/diphtheria toxin receptor *HBEGF/DTR*

(Iwamoto et al., 1994; Naglich et al., 1992) linked to the mCherry gene via a sequence for a *2a* self-cleaving peptide linker. The entire DTR-2a-mCherry flanked by restriction enzyme sequences BamHI and XhoI was synthesized at Eurofins Genomics. EEV plasmid was purified using the EndoFree Plasmid Maxi Kit (Qiagen #12362). A total of 200,000 cells were resuspended in buffer T, mixed with 0.5–3 μg DNA, and electroporated (Neon Transfection System; settings: 990 V, 40 ms, 1 pulse). The cells were transferred to culture dishes and used for transplantation after 48 h of culture. Transfection efficiency was performed by visualizing the mCherry fluorescence (Figures 7B and 7C1–7C4). To deplete the transplanted NPCs, we injected rats with 100 mg/kg DT intraperitoneally (i.p.) once daily for 3 days.

Sacrifice and Harvesting of Spinal Cords and NPCs

Rats were euthanized with 20% CO_2 followed by decapitation when harvesting brains for SVZ extraction. When harvesting spinal cords, the rats were given a lethal dose of pentobarbital i.p. followed by transcardial perfusion using 1× PBS with a peristaltic pump (Autoclude). Spinal cords subject to gene expression analysis were dissected, snap-frozen in liquid nitrogen, and stored at −70°C until analysis. Spinal cords from which transplanted NPCs were to be isolated using fluorescence-activated cell sorting (FACS) were dissected following perfusion with 1× PBS. Animals subjected to histological evaluation of the spinal cord were perfused with 4% paraformaldehyde (PFA) following perfusion with 1× PBS. These spinal cords were then post-fixated in 4% PFA for 24 h at 4°C prior to cryoprotection.

## Cerebrospinal Fluid Collection and Immunoassay

CSF was collected when the animals were fully euthanized. Using a safety winged IV needle (Venofix Safety #4056501-01) and a 1-mL syringe, the CSF was aspirated from the cisterna magna. CSF was collected, snap-frozen in liquid nitrogen, and stored at −70°C until analysis. Expression of cytokines/chemokines was assessed by a Bio-Plex Pro Rat Cytokine 24-plex Assay kit (Bio-Rad #10014905) using 25 μL of CSF from each animal as per manufacturer's instructions.

Immunohistochemistry and Immunocytochemistry

Spinal cords were cryoprotected in 15% followed by 30% sucrose (Sigma #S9378) in 1× PBS. Transverse sections (14 μm) were produced using a cryostat (Leica #CM1850) and mounted on adhesion slides (SuperFrost Plus; VWR #48,311-703). Sections were thawed at room temperature (RT) for 20 min and rehydrated

Figure 6. Recovery of Hindlimb Motor Function and Coordination

(A) Experimental design.

(B) Basso, Beattie, and Bresnahan (BBB) locomotor rating scale over time. Mean surrounded by a 95% CI. Each dot represents one animal. Significance of post hoc test between SCI+NPC and SCI+saline are reported (*p < 0.05; ns, not significant).

(C) Iliac crest height over time. Data reporting and statistics as in (B).

(D) Number of forelimb steps taken on an 80-cm runway. Data reporting and statistics as in (B).

(E) Protraction (positive distance) and retraction (negative distance) over time. Data reporting and statistics as in (B).

(F and G) Stride width (F) and stride length (G). Data reporting and statistics as in (B), except that the circles are centered on the mean value and their radius is the standard deviation.

(H) Placement of the hindlimb paws (average x/y coordinate per treatment group).
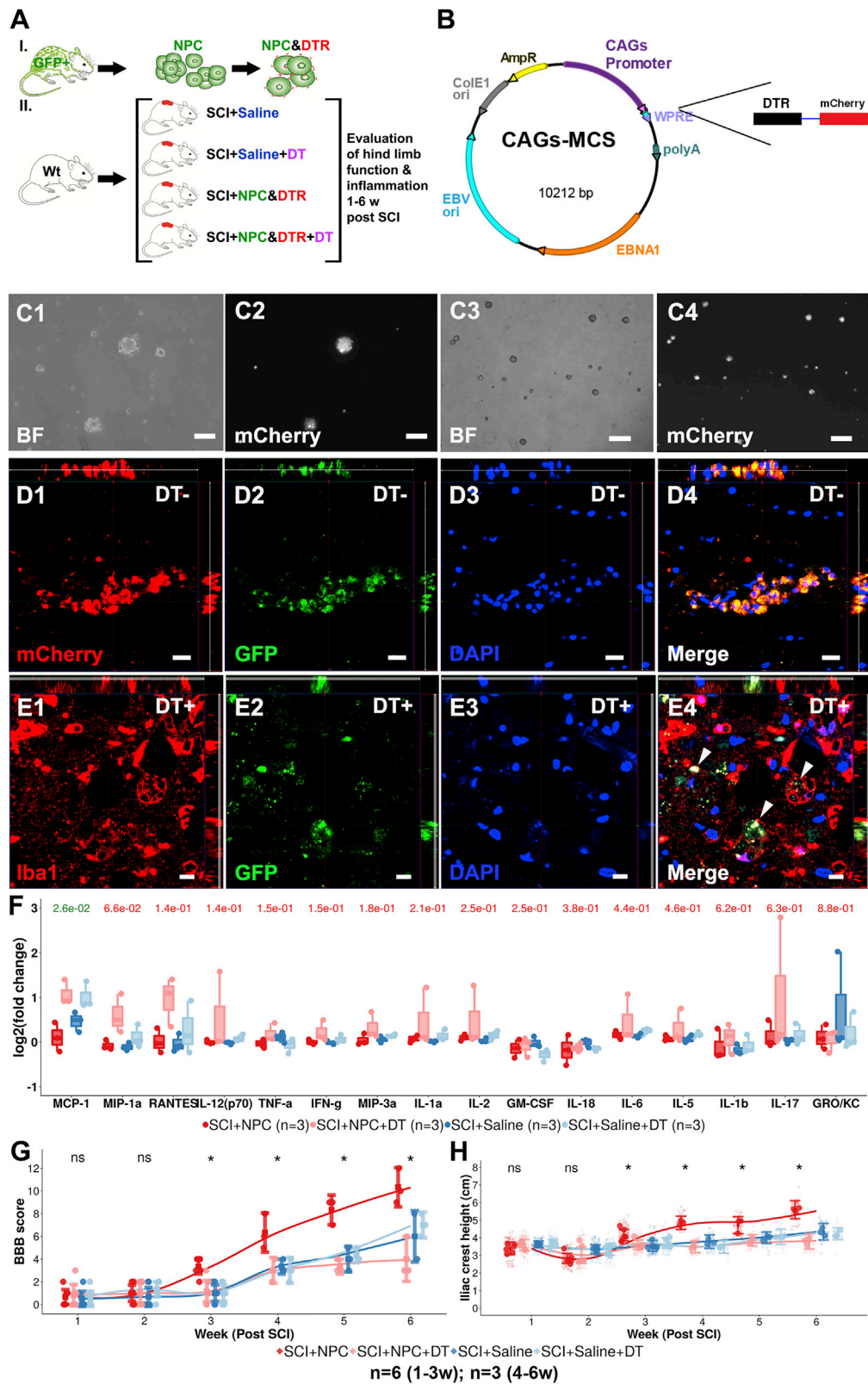
(legend on next page)

in 1× PBS at RT for 10 min. Primary antibody (Table S4) was diluted in blocking buffer (3% BSA, 5% normal donkey serum, 0.3% Triton X-100, 0.01% Na Azide, 1× PBS) and added onto the slides and incubated overnight at 4°C. Sections were washed and secondary antibody was added (Table S4), and the sections were incubated for 45 min at RT. Sections were washed with 1× PBS containing Hoechst 33258 (2 μg/mL) or DAPI or 10–15 min at RT. Sections were washed and mounted. NPCs cultured or differentiated on coated glass slides in a 24-well plate were fixated, stained, and prepared for imaging using the same protocol as for the thin spinal cord sections. Sections were imaged using a confocal microscope (Zeiss LSM 880 Airyscan and Leica SP5) or a stereomicroscope (Leica MZ95).

Survival rate of transplanted NPCs was estimated by multiplying the average number of GFP+ NPCs per section times the number of 16-μm sections 3 mm in the caudal and cranial direction of the epicenter (6,000 μm/[16 μm/section] = 375 sections). This number was then divided by the total number of transplanted NPCs in each animal. The differentiation profile of transplanted NPCs was quantified by counting all GFP+ and Sox2+/CC1+/TuJ1+/GFAP+ cells in four random sections per animal in four transplanted animals. The percentage was estimated by dividing all cells that were double-positive for either Sox2, CC1, TuJ1, or GFAP and GFP with the total number of GFP+ cells. Quantification was done by manual counting using 40/63× magnification.

Luxol Fast Blue Staining

Sections were rehydrated in 1× PBS for 15 min followed by hydration in 95% EtOH for 15 min. Sections were placed in a cuvette and incubated in 0.1% Luxol fast blue solution (0.1 mg of Luxol fast blue [Waldeck #1B-389], 100 mL of 95% EtOH, and 0.5 mL of glacial acetic acid [Millipore]) at 56°C overnight. Excess stain was removed using 95% EtOH followed by rinse in dH$_2$O. Slides were differentiated in 0.05% lithium carbohydrate solution (0.05 mg of lithium carbonate [Karolinska apoteket #941122], 100 mL of dH$_2$O) for 30 s followed by differentiation in 70% EtOH for 30 s and rinsed in dH$_2$O. Sections were mounted using xylene (VWR) and imaged using a light microscope (Leica Reichert Polyvar 2).

Locomotor and Kinematic Assessment of Hindlimb Function

A custom-made apparatus allowing for continuous recording of walking across a runway was constructed using Plexiglas and mirrors. Walking was recorded using a camera (Canon EOS 6D). The (1) iliac crest, (2) greater trochanter, (3) lateral malleolus, (4) metatarsophalangeal joint of the fifth toe, and (5) tip of the toe were labeled. Footsteps were recorded by illuminating the glass surface on the bottom of the runway with LED light. All recordings were analyzed using specialized software (Click Joint; AEA solutions) (Zorner et al., 2010). In addition to the kinematic evaluation, the open-field behavioral outcome was assessed using the BBB locomotor rating scale (Basso et al., 1995).

Isolation of Transplanted Neural Progenitor Cells

NPCs were isolated from injured and uninjured spinal cord using FACS. The spinal cords were dissociated in 10 U/mL papain (Worthington #L5003126). Myelin was removed using 30% Percoll in 1× Dulbecco's PBS (Sigma #P1644). Remaining tissue was filtered consecutively through pre-wet 100-μm and 40-μm cell strainers. Tissue was washed and resuspended in FACS buffer (1% BSA [Sigma #A8412], 2 mM EDTA [Gibco #15575-038], 25 mM HEPES [Sigma #H0887]). A BD Influx cell sorter was used for isolation (Figures S7A and S7B). Isolated cells were collected by centrifugation at 300 × g for 5 min, resuspended in 1 mL of TRIzol reagent (Thermo Fisher #15596026), vortexed, and stored at −70°C until RNA isolation. Non-transplanted NPCs were exposed to the FACS procedure prior to RNA isolation.

RNA Extraction and Cleanup

Total RNA was isolated from spinal cord tissue and isolated NPCs. RNA from spinal cord (15 mg) was isolated with RNeasy mini kit (Qiagen #74104). In the process the tissue was mechanically dissociated (TissueLyser LT, Qiagen) in lysis buffer (Qiagen) supplemented with 1% β-mercaptoethanol, and contamination genomic DNA was eliminated by on-column digestion using DNase (DNase I, Qiagen #79254). RNA from isolated NPCs was extracted using TRIzol reagent (Thermo Fisher #15596026). Isopropanol precipitation was performed overnight using 75 μg of glycogen (Invitrogen #AM9516). Cleanup was performed using RNeasy micro kit (Qiagen #74004). The RNA was stored at −70°C until analysis.

Sequencing RNA from Isolated Neural Progenitor Cells

Sequencing libraries for RNA from isolated NPCs were prepared using SMARTer Stranded Total RNA-Seq Kit—Pico Input Mammalian

---

Figure 7. Active Elimination of Transplanted NPCs
(A) Experimental design.
(B) Enhanced episomal cloning and expression vector used for diphtheria toxin (DT) receptor insertion.
(C) mCherry+ NPCs in bright field (BF) and with red fluorescence filter (C1–C4). Scale bars, 50 μm.
(D) mCherry+GFP+ NPCs following transplantation into SCI (D1–D4). Scale bars, 20 μm.
(E) GFP+ NPCs following transplantation into SCI (E1–E4). Scale bars, 10 μm.
(F) Expression of cytokines/chemokines in the cerebrospinal fluid (CSF) as log$_2$(fold change) to expression in healthy animals. Each dot represents one animal. p values for two-group comparison between SCI+NPC and SCI+NPC and DT are presented.
(G) BBB locomotor rating scale over time. Data reporting and statistics as in (F) except that 95% CIs are provided instead of box plots (*p < 0.05; ns, not significant).
(H) Iliac crest height over time. Data reporting and statistics as in (G). Technical replicates are reported as diamonds.
See also Figure S6.

(Clontech) from total RNA. Libraries were sequenced 2 × 125 bp on two lanes using HiSeq2500 (Illumina) on high-output mode. For each replicate, a minimum of $(188 \times 10^6 \times 2)/28 = 13.4 \times 10^6$ read-pairs were used. TrimGalore (Babraham Bioinformatics) was used for removal of low-quality regions and adapter sequences. Read-pairs were aligned to a rat reference genome (Rnor_6.0) using STAR. featureCounts and Ensembl annotation release 81 were used for summary of read counts over genes. Differential gene expression analysis was conducted in R (version 3.5.1) using packages "limma" and "edgeR." Functional analysis was conducted using "WebGestaltR" using over-representation enrichment analysis and network topology-based analysis. Up- and downregulated genes (false discovery rate [FDR] < 0.01; $\log_{FC} = 1$) in each contrast were analyzed. All GO and Kyoto Encyclopedia of Genes and Genomes (KEGG) terms that fulfilled FDR < 0.01 were exported. General categories were then created into which the GO/KEGG terms were categorized. Median FDR for GO/KEGG terms and the FDR following competitive gene set testing was determined for each category. Categories in which both FDRs fulfilled <0.05 were deemed significant. The GEO accession number for data is GEO: GSE125134.

Statistical Analysis

Data were presented as mean with 95% CI or median with range (25th and 75th percentile). p values of <0.05 were considered significant. When possible, technical and biological replicates were presented in combination with summary statistics. Assumptions of normality and homogeneity of variances were evaluated using the Shapiro-Wilk test and Fligner-Killeen test, respectively. Independent two-group comparisons were conducted using Student's t test with or without Welch's correction or using a Wilcoxon rank-sum test. A mixed ANOVA was implemented for cases with one independent variable and one dependent variable. Main effects were investigated using one-way ANOVA (with or without repeated measures) for each variable. One-way ANOVA was supplemented with post hoc comparisons using Tukey's honest significant difference test. Statistical analysis was conducted and graphical presentation prepared by R (version 3.5.1).

SUPPLEMENTAL INFORMATION

Supplemental Information can be found online at https://doi.org/10.1016/j.stemcr.2019.03.013.

AUTHOR CONTRIBUTIONS

Experimental design: S.R.S., R.H., R.C., M.S., and L.B. Animal care, breeding, genotyping, spinal cord injury, transplantation: S.R.S. Sacrifice, tissue harvesting: S.R.S., R.H., A.F., and S.N. Cell culture: S.R.S. and R.C. Immunohistochemistry and confocal microscopy: S.R.S. and R.H. Light sheet fluorescence microscopy: S.R.S., R.H., and A.F. Assessment of locomotor function: S.R.S. and R.H. Fluorescence activated cell sorting: S.R.S. and R.H. RNA extraction and clean-up, reverse transcription and RT-qPCR: S.R.S. and R.H. RNA-sequencing: S.R.S. and R.H. Statistical analysis, graphical presentation: R.H. and S.R.S. Manuscript writing and editing: S.R.S., R.H., M.S., L.B., R.C., A.F., and S.N.

REFERENCES

Ahuja, C.S., Wilson, J.R., Nori, S., Kotter, M.R.N., Druschel, C., Curt, A., and Fehlings, M.G. (2017). Traumatic spinal cord injury. Nat. Rev. Dis. Primers 3, 17018.

Akesson, E., Piao, J.H., Samuelsson, E.B., Holmberg, L., Kjaeldgaard, A., Falci, S., Sundström, E., and Seiger, A. (2007). Long-term culture and neuronal survival after intraspinal transplantation of human spinal cord-derived neurospheres. Physiol. Behav. 92, 60–66.

Amemori, T., Romanyuk, N., Jendelova, P., Herynek, V., Turnovcova, K., Prochazka, P., Kapcalova, M., Cocks, G., Price, J., and Sykova, E. (2013). Human conditionally immortalized neural stem cells improve locomotor function after spinal cord injury in the rat. Stem Cell Res. Ther. 4, 68.

Basso, D.M., Beattie, M.S., and Bresnahan, J.C. (1995). A sensitive and reliable locomotor rating scale for open field testing in rats. J. Neurotrauma 12, 1–21.

Ben-Hur, T. (2010). Reconstructing neural circuits using transplanted neural stem cells in the injured spinal cord. J. Clin. Invest. 120, 3096–3098.

Boido, M., Garbossa, D., and Vercelli, A. (2011). Early graft of neural precursors in spinal cord compression reduces glial cyst and improves function. J. Neurosurg. Spine 15, 97–106.

Bonner, J.F., Connors, T.M., Silverman, W.F., Kowalski, D.P., Lemay, M.A., and Fischer, I. (2011). Grafted neural progenitors integrate and restore synaptic connectivity across the injured spinal cord. J. Neurosci. 31, 4675–4686.

Brock, J.H., Graham, L., Staufenberg, E., Im, S., and Tuszynski, M.H. (2017). Rodent neural progenitor cells support functional recovery after cervical spinal cord contusion. J. Neurotrauma 35, 1069–1078.

Cheng, Z., Zhu, W., Cao, K., Wu, F., Li, J., Wang, G., Li, H., Lu, M., Ren, Y., and He, X. (2016). Anti-inflammatory mechanism of neural stem cell transplantation in spinal cord injury. Int. J. Mol. Sci. 17. https://doi.org/10.3390/ijms17091380.

Covacu, R., Perez Estrada, C., Arvidsson, L., Svensson, M., and Brundin, L. (2014). Change of fate commitment in adult neural progenitor cells subjected to chronic inflammation. J. Neurosci. 34, 11571–11582.

Cummings, B.J., Uchida, N., Tamaki, S.J., and Anderson, A.J. (2006). Human neural stem cell differentiation following transplantation into spinal cord injured mice: association with recovery of locomotor function. Neurol. Res. 28, 474–481.

Cummings, B.J., Uchida, N., Tamaki, S.J., Salazar, D.L., Hoosh-mand, M., Summers, R., Gage, F.H., and Anderson, A.J. (2005). Human neural stem cells differentiate and promote locomotor recovery in spinal cord-injured mice. Proc. Natl. Acad. Sci. U S A *102*, 14069–14074.

Curtis, E., Martin, J.R., Gabel, B., Sidhu, N., Rzesiewicz, T.K., Mandeville, R., Van Gorp, S., Leerink, M., Tadokoro, T., Marsala, S., et al. (2018). A first-in-human, phase i study of neural stem cell transplantation for chronic spinal cord injury. Cell Stem Cell *22*, 941–950.e946.

Cusimano, M., Biziato, D., Brambilla, E., Donegà, M., Alfaro-Cervello, C., Snider, S., Salani, G., Pucci, F., Comi, G., Garcia-Verdugo, J.M., et al. (2012). Transplanted neural stem/precursor cells instruct phagocytes and reduce secondary tissue damage in the injured spinal cord. Brain *135*, 447–460.

Doetsch, F., Caille, I., Lim, D.A., Garcia-Verdugo, J.M., and Alvarez-Buylla, A. (1999). Subventricular zone astrocytes are neural stem cells in the adult mammalian brain. Cell *97*, 703–716.

Fujimoto, Y., Abematsu, M., Falk, A., Tsujimura, K., Sanosaka, T., Juliandi, B., Semi, K., Namihira, M., Komiya, S., Smith, A., et al. (2012). Treatment of a mouse model of spinal cord injury by transplantation of human induced pluripotent stem cell-derived long-term self-renewing neuroepithelial-like stem cells. Stem Cells *30*, 1163–1173.

Gu, Y.L., Yin, L.W., Zhang, Z., Liu, J., Liu, S.J., Zhang, L.F., and Wang, T.H. (2012). Neurotrophin expression in neural stem cells grafted acutely to transected spinal cord of adult rats linked to functional improvement. Cell Mol. Neurobiol. *32*, 1089–1097.

Hofstetter, C.P., Holmström, N.A., Lilja, J.A., Schweinhardt, P., Hao, J., Spenger, C., Wiesenfeld-Hallin, Z., Kurpad, S.N., Frisén, J., and Olson, L. (2005). Allodynia limits the usefulness of intraspinal neural stem cell grafts; directed differentiation improves outcome. Nat. Neurosci. *8*, 346–353.

Hong, J.Y., Lee, S.H., Lee, S.C., Kim, J.W., Kim, K.P., Kim, S.M., Tapia, N., Lim, K.T., Kim, J., Ahn, H.S., et al. (2014). Therapeutic potential of induced neural stem cells for spinal cord injury. J. Biol. Chem. *289*, 32512–32525.

Iwamoto, R., Higashiyama, S., Mitamura, T., Taniguchi, N., Klagsbrun, M., and Mekada, E. (1994). Heparin-binding EGF-like growth factor, which acts as the diphtheria toxin receptor, forms a complex with membrane protein DRAP27/CD9, which up-regulates functional receptors and diphtheria toxin sensitivity. EMBO J. *13*, 2322–2330.

Jin, Y., Bouyer, J., Shumsky, J.S., Haas, C., and Fischer, I. (2016). Transplantation of neural progenitor cells in chronic spinal cord injury. Neuroscience *320*, 69–82.

Johansson, C.B., Momma, S., Clarke, D.L., Risling, M., Lendahl, U., and Frisén, J. (1999). Identification of a neural stem cell in the adult mammalian central nervous system. Cell *96*, 25–34.

Karimi-Abdolrezaee, S., Eftekharpour, E., Wang, J., Morshead, C.M., and Fehlings, M.G. (2006). Delayed transplantation of adult neural precursor cells promotes remyelination and functional neurological recovery after spinal cord injury. J. Neurosci. *26*, 3377–3389.

Kulbatski, I., and Tator, C.H. (2009). Region-specific differentiation potential of adult rat spinal cord neural stem/precursors and their plasticity in response to in vitro manipulation. J. Histochem. Cytochem. *57*, 405–423.

Kumamaru, H., Ohkawa, Y., Saiwai, H., Yamada, H., Kubota, K., Kobayakawa, K., Akashi, K., Okano, H., Iwamoto, Y., and Okada, S. (2012). Direct isolation and RNA-seq reveal environment-dependent properties of engrafted neural stem/progenitor cells. Nat. Commun. *3*, 1140.

Kumamaru, H., Saiwai, H., Kubota, K., Kobayakawa, K., Yokota, K., Ohkawa, Y., Shiba, K., Iwamoto, Y., and Okada, S. (2013). Therapeutic activities of engrafted neural stem/precursor cells are not dormant in the chronically injured spinal cord. Stem Cells *31*, 1535–1547.

Li, Z., Guo, G.H., Wang, G.S., Guan, C.X., and Yue, L. (2014). Influence of neural stem cell transplantation on angiogenesis in rats with spinal cord injury. Genet. Mol. Res. *13*, 6083–6092.

Lu, P., Wang, Y., Graham, L., McHale, K., Gao, M., Wu, D., Brock, J., Blesch, A., Rosenzweig, E.S., Havton, L.A., et al. (2012). Long-distance growth and connectivity of neural stem cells after severe spinal cord injury. Cell *150*, 1264–1273.

Macias, M.Y., Syring, M.B., Pizzi, M.A., Crowe, M.J., Alexanian, A.R., and Kurpad, S.N. (2006). Pain with no gain: allodynia following neural stem cell transplantation in spinal cord injury. Exp. Neurol. *201*, 335–348.

Mligiliche, N.L., Xu, Y., Matsumoto, N., and Idel, C. (2005). Survival of neural progenitor cells from the subventricular zone of the adult rat after transplantation into the host spinal cord of the same strain of adult rat. Anat. Sci. Int. *80*, 229–234.

Morshead, C.M., Reynolds, B.A., Craig, C.G., McBurney, M.W., Staines, W.A., Morassutti, D., Weiss, S., and van der Kooy, D. (1994). Neural stem cells in the adult mammalian forebrain: a relatively quiescent subpopulation of subependymal cells. Neuron *13*, 1071–1082.

Naglich, J.G., Metherall, J.E., Russell, D.W., and Eidels, L. (1992). Expression cloning of a diphtheria toxin receptor: identity with a heparin-binding EGF-like growth factor precursor. Cell *69*, 1051–1061.

Nishimura, S., Yasuda, A., Iwai, H., Takano, M., Kobayashi, Y., Nori, S., Tsuji, O., Fujiyoshi, K., Ebise, H., Toyama, Y., et al. (2013). Time-dependent changes in the microenvironment of injured spinal cord affects the therapeutic potential of neural stem cell transplantation for spinal cord injury. Mol. Brain *6*, 3.

Okada, S., Ishii, K., Yamane, J., Iwanami, A., Ikegami, T., Katoh, H., Iwamoto, Y., Nakamura, M., Miyoshi, H., Okano, H.J., et al. (2005). In vivo imaging of engrafted neural stem cells: its application in evaluating the optimal timing of transplantation for spinal cord injury. FASEB J. *19*, 1839–1841.

Pallini, R., Vitiani, L.R., Bez, A., Casalbore, P., Facchiano, F., Di Giorgi Gerevini, V., Falchetti, M.L., Fernandez, E., Maira, G., Peschle, C., et al. (2005). Homologous transplantation of neural stem cells to the injured spinal cord of mice. Neurosurgery *57*, 1014–1025, discussion 1014–1025.

Parr, A.M., Kulbatski, I., and Tator, C.H. (2007). Transplantation of adult rat spinal cord stem/progenitor cells for spinal cord injury. J. Neurotrauma *24*, 835–845.

Pfeifer, K., Vroemen, M., Blesch, A., and Weidner, N. (2004). Adult neural progenitor cells provide a permissive guiding substrate for corticospinal axon growth following spinal cord injury. Eur. J. Neurosci. *20*, 1695–1704.

Pfeifer, K., Vroemen, M., Caioni, M., Aigner, L., Bogdahn, U., and Weidner, N. (2006). Autologous adult rodent neural progenitor cell transplantation represents a feasible strategy to promote structural repair in the chronically injured spinal cord. Regen. Med. *1*, 255–266.

Piltti, K.M., Salazar, D.L., Uchida, N., Cummings, B.J., and Anderson, A.J. (2013). Safety of human neural stem cell transplantation in chronic spinal cord injury. Stem Cells Transl. Med. *2*, 961–974.

Reynolds, B.A., and Weiss, S. (1992). Generation of neurons and astrocytes from isolated cells of the adult mammalian central nervous system. Science *255*, 1707–1710.

Ricci-Vitiani, L., Casalbore, P., Petrucci, G., Lauretti, L., Montano, N., Larocca, L.M., Falchetti, M.L., Lombardi, D.G., Gerevini, V.D., Cenciarelli, C., et al. (2006). Influence of local environment on the differentiation of neural stem cells engrafted onto the injured spinal cord. Neurol. Res. *28*, 488–492.

Salazar, D.L., Uchida, N., Hamers, F.P., Cummings, B.J., and Anderson, A.J. (2010). Human neural stem cells differentiate and promote locomotor recovery in an early chronic spinal cord injury NOD-scid mouse model. PLoS One *5*, e12272.

Salewski, R.P., Mitchell, R.A., Shen, C., and Fehlings, M.G. (2015). Transplantation of neural stem cells clonally derived from embryonic stem cells promotes recovery after murine spinal cord injury. Stem Cells Dev. *24*, 36–50.

Sandhu, M.S., Ross, H.H., Lee, K.Z., Ormerod, B.K., Reier, P.J., and Fuller, D.D. (2017). Intraspinal transplantation of subventricular zone-derived neural progenitor cells improves phrenic motor output after high cervical spinal cord injury. Exp. Neurol. *287*, 205–215.

Tepavčević, V., Lazarini, F., Alfaro-Cervello, C., Kerninon, C., Yoshikawa, K., Garcia-Verdugo, J.M., Lledo, P.M., Nait-Oumesmar, B., and Baron-Van Evercooren, A. (2011). Inflammation-induced subventricular zone dysfunction leads to olfactory deficits in a targeted mouse model of multiple sclerosis. J. Clin. Invest. *121*, 4722–4734.

Vroemen, M., Aigner, L., Winkler, J., and Weidner, N. (2003). Adult neural progenitor cell grafts survive after acute spinal cord injury and integrate along axonal pathways. Eur. J. Neurosci. *18*, 743–751.

Yokota, K., Kobayakawa, K., Kubota, K., Miyawaki, A., Okano, H., Ohkawa, Y., Iwamoto, Y., and Okada, S. (2015). Engrafted neural stem/progenitor cells promote functional recovery through synapse reorganization with spared host neurons after spinal cord injury. Stem Cell Reports *5*, 264–277.

Zorner, B., Filli, L., Starkey, M.L., Gonzenbach, R., Kasper, H., Rothlisberger, M., Bolliger, M., and Schwab, M.E. (2010). Profiling locomotor recovery: comprehensive quantification of impairments after CNS damage in rodents. Nat. Methods *7*, 701–708.